Proceedings of Hydraulic Engineering,
JSCE VOL. 37 (1993)

Multiple Instability of a Laboratory Stratified Shear Layer

Colm-cille P. Caulfield*and Shizuo Yoshida**

The behaviour of a stratified shear flow with a three layer density distribution is investigated both theoretically and experimentally. Three distinct types of instability are observed in accordance with the predictions of linear theory. The most important parameter for the selection of the particular type of instability is found to be the ratio R of the depth of the intermediate density layer to the depth over which the velocity varies, though any asymmetry in the flow (either in the velocity or density fields) also plays a role. In general all three instabilities can be observed simultaneously at markedly different wavelengths and phase speeds for significant periods of time, although linear theory predicts very different growthrates.The development of the various instabilities can be simply and intuitively interpreted in terms of interactions of interfacial waves, and at finite amplitude each type of instability has a different structure and mixes the flow in a qualitatively different manner.

Keywords: stratified flow, interfacial instability, eigenvalue equation

1. Theoretical Introduction

In the immediate vicinity of a river mouth, much mixing takes place due to the sudden widening of the channel that the river flows along. This mixing between the river and sea water can lead to a three layer density structure that is then sheared by the salt wedge and river counterflow.

The first theoretical investigation of a flow with a three layer density field was conducted by Taylor (1931). This was at the extreme of a three layer density field with the intermediate layer the same depth as the region of velocity variation. For all Ri, this flow exhibits overturnings in the intermediate layer, which propagate at the mean velocity of the background flow. As Taylor states, these overturnings can be thought of as arising from resonances of two gravity waves, one on each of the density interfaces. This instability has not been observed experimentally.

We wish to consider a flow with a three layer density distribution, but *a priori* we make no assumption about any symmetries between the density field and the velocity field. In particular, we do not assume that the intermediate layer has density equal to the mean of the other two layers. We briefly reiterate the discussion of Caulfield (1991), where further details may be found. We assume that the background flow is as shown in figure 1. The velocity profile is piecewise linear over a depth d. Four non-dimensional parameters that describe the nature of the velocity and density distributions are defined as

$$Ri_0 \equiv \frac{g(\rho_3-\rho_1)}{\Delta U^2}, \qquad R \equiv \frac{\delta}{d}, \qquad \beta \equiv \frac{2h}{d}, \qquad \Theta \equiv \frac{\rho_2-\rho_1}{\rho_3-\rho_1}.$$

Ri_0 is the bulk Richardson number. R is a measure of the relative depths of the intermediate density layer to the depth of the shear layer. The parameter β is the three layer generalisation of the parameter ε used by Lawrence *et al.* (1991) to quantify the asymmetry in a two layer flow system. In our work, β is a measure of asymmetry in the *location* of the density field *relative* to the velocity field, while the parameter Θ is a measure of the asymmetry in the *distribution* of the density field. It is important to note that in general β can be negative, while R and Θ must be between 0 and 1. In our calculations, we assume that $|\beta| + R \leq 1$, and hence that the region of intermediate density is entirely contained within the region of

* Department of Physics, University of Toronto, 60 St George Street, Toronto M5S 1A7 Canada
** Shizuo Yoshida, Department of Engineering Science, Hokkaido University, Sapporo 060

varying velocity. This situation is thought to be the most physically likely. Relaxing this condition changes the governing equations slightly, but does not change the results significantly. By classical normal mode methods of matching pressure and vertical disturbance across interfaces, we may derive a sixth order eigenvalue equation for the phase speed $c = c_r + ic_i$,

$$c^6 + a_1 c^5 + a_2 c^4 + a_3 c^3 + a_4 c^2 + a_5 c + a_6 = 0 , \qquad (1)$$

where the a_i are well defined functions of α, the non-dimensional wavenumber (i.e $\alpha = k\,d/2$), Ri_0, R, β and Θ. The flow is unstable if $c_i > 0$, with growthrate αc_i. As (1) is in general a sextic, we expect that, in general, the equation will have six, complex roots. The equation is solved using the IMSL root finding algorithm DZPLRC. In figure 2, the real parts of these roots (i.e. the phase speed c_r) are plotted with solid lines against α, for typical experimental background values of Ri_0, R, β and Θ, namely Ri_0=1.5, R=0.4, β=0.05 and Θ=0.5. Note that for $\alpha < 0.23$, two of the roots have real phase speed with magnitude greater than 1, and so do not appear on the graph. Regions of instability correspond to regions where two of the roots have the same phase speed and wavenumber. In this case, one of the roots is damped and the other one is predicted to grow. In figure 3 we plot the growth rates αc_i, of the various modes against α for the same parameters as figure 2. Note that there is a marked difference in the growthrates between the various types of instability. These growthrates are calculated numerically, directly from equation (1).

The dashed lines represent the various waves that would exist on each of the interfaces if they were totally isolated, which corresponds to a large α limit. We see that each of the regions of instability can be thought of as arising from an interaction of these various waves.

The small real phase instability for $4.57 \leq \alpha \leq 4.8$ occurs when there is an interaction between the internal wave on the upper density interface that is travelling upstream relative to the background flow, and the internal wave on the lower density interface that is also travelling upstream relative to the background flow. This corresponds to an $R \neq 1$ asymmetric generalisation of the situation first considered by Taylor (1931), and we shall henceforth refer to this as a K mode.

The two regions of large real phase speed instability ($2.55 \leq \alpha \leq 3.45$ and $3.54 \leq \alpha \leq 4.44$) correspond to the asymmetric three layer generalisation of the modes first considered by Holmboe (1962), and we shall refer to them as the HP and HM modes respectively. They are caused by interactions between upstream propagating Rayleigh waves and downstream propagating gravity waves on the nearer density interface. Both are locally driven.

There is the possibility of two further regions of instability at small wavenumber, if the Rayleigh waves resonate with the gravity waves on the further density interface. These are non-local interactions, which we refer to as R modes. For the parameters chosen for figure 2, the full calculations show that the R type modes are unstable for $0.54 \leq \alpha \leq 0.65$. Here, the large α approximation used in the derivation of the interfacial waves is not, strictly speaking, valid. Indeed, there is a slight difference between the crossing of the interfacial waves, when their phase speed as a function of wavenumber is calculated separately for each interface, and the crossing for the roots of the full equation (1).

In figure 4, we plot the regions of instability predicted by (1) in Ri_0-α space along with the resonance conditions for the various wave interactions for β=0.05, R=0.4, and Θ=1/2. Each branch ultimately asymptotes to the appropriate predicted resonance, provided Ri_0 (and hence α) is sufficiently large.

The relative significance of the various branches varies as the various parameters change. The most significant effect is that the K mode moves to larger α and smaller growthrate as R decreases, while the Holmboe type modes start to dominate. Positive (negative) β, or $\Theta < (>)$ 1/2 decreases (increases) the wavenumber of the HP modes relative to that of the HM mode, and increases (decreases) the HP mode growthrate. The R modes are only significant at small R.

Thus, a simple consideration of the various interfaces separately sheds valuable insights

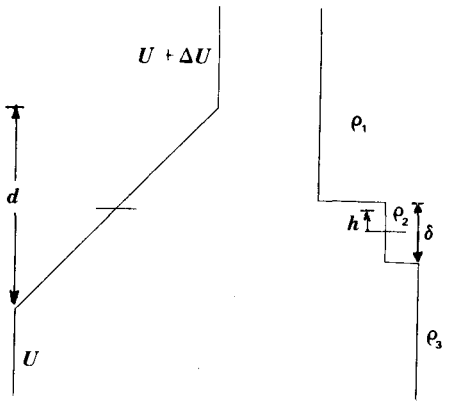

Figure 1: Model background velocity and density distributions, for R=0.3, β =0.2 andΘ =2/3.

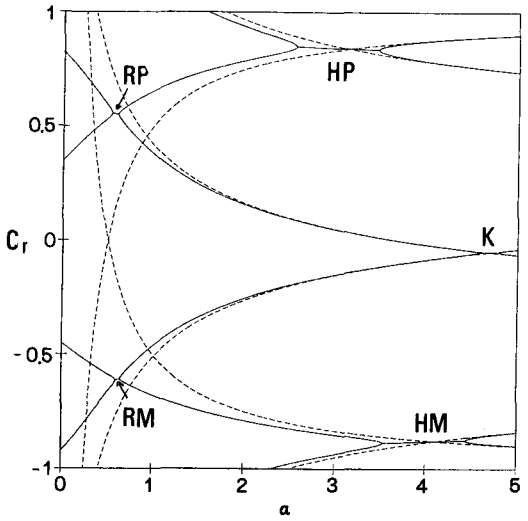

Figure 2: Phase speed against wavenumber for the full solutions (solid lines) of (1) for Ri_0=1.5, R=0.4, β =0.05 and Θ =1/2. Instability corresponds to two roots of (1) with the same real phase speed. The phase speeds of the waves on each of the interfaces considered separately are shown as dashed lines.

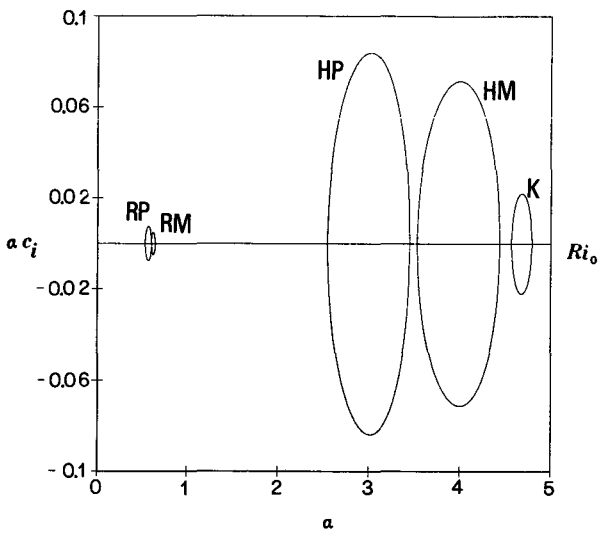

Figure 3: Growthrate against wavenumber for the full solutions of (1) for Ri_0 =1.5, R =0.4, β =0.05 and Θ =1/2. At instability, note the presence of damped solutions also.

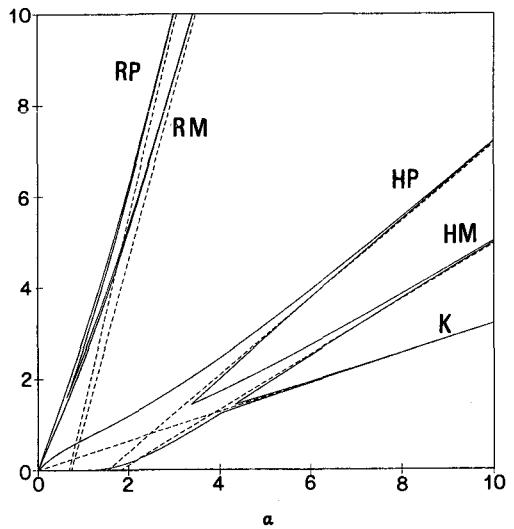

Figure 4: Stability boundary (solid line) for R=0.4, β =0.05, Θ =1/2. The resonant conditions for the various interfacial waves are shown as dashed lines. Note that all the branches asymptote to the correct resonance conditions.

on the growth mechanisms, phase speeds and wavelengths of the different types of instability predicted by the full linear model.

2.Experimental Results

Twenty four experiments were conducted in a flume 8 metres long by 50 cm wide with a terminal reservoir 2 metres long by 3 metres wide by 10 cm deep. (see Yoshida 1986 for a description of the tank). The flume (modelling a river) was filled with a saline solution to a depth of 4 or 6 cm. This initial depth variation had little effect on the subsequent evolution of the flow. A less dense, though still salty layer, dyed with Sodium Fluorescein (Uranine or $C_{20}\,H_{10}\,Na_2\,O_2$) was then introduced, until the total depth became 10 cm and the reservoir (representing the sea) overflowed. A constant flux of fresh water was then introduced at the upstream end. A constant flux was also introduced to the flexible impermeable floor of the reservoir, and hence both the lower layer and upper layer had non-zero velocities, and a roughly linear velocity shear existed across the entirety of the intermediate dyed layer.

The evolution of the velocity field throughout the whole depth of the tank was tracked through time using image analysis of dye streaks, calibrated at two points by a laser Doppler velocimeter (LDV). R varied markedly through one experiment. An advantage of driving both upper and lower layers was that, after initial transient effects due to the filling of the tank, the two density interfaces became very sharp. From conductivity measurements, the interfacial width was found to be o(2 mm). Various values of flow rate, ρ_3 and ρ_2 were chosen to allow for variation in background flow parameter values. Experimentally, $1.03 \leq Ri_0 \leq 2.83$, $0.1 \leq R \leq 0.78$, $-0.34 \leq \beta \leq 0.19$ and $0.25 \leq \Theta \leq 0.75$. Eighty nine well-defined unstable structures were observed, by means of a centrally located lightsheet about 50 cm from the reservoir-flume channel junction, with three qualitatively different finite amplitude structures. Firstly, especially near the beginning of experiments (when R was close to 1) disturbances on the two density interfaces locked in phase, the interfaces cusped inwards, and regions of overturning appeared within the intermediate density region. These disturbances propagated at phase speeds close to the mean velocity of the flow, and we identified these as K mode type disturbances (Photogragh 1). In figure 5, we plot observed wavenumber for these overturnings with the wavenumber region predicted by the modeldescribed in the previous section to be unstable to K mode type disturbances. We see that there is a very close agreement, as there is in phase speed, though we do not plot that here. Thus we have observed the K mode, and we also see the predicted transition to larger wavenumber as R decreases. The K mode overturnings were found to be strongly two dimensional, and though the overturnings were longlived within the intermediate layer, very little fluid was entrained from the other two layers, and hence the K mode did not contribute greatly to the mixing. This is not entirely a surprise, as Ri_0 is of order 1 here, and thus the mixing effects of Kelvin-Helmholtz type billows is thought to be severely suppressed.

Also observed is a cusping upwards of the upper density interface, associated with the presence of a region of overturning in the upper layer. These disturbances typically have phase speed less than, but close to, the maximum velocity of the background flow. In figure 6, we plot observed wavenumber for these overturnings with the wavenumber region predicted by the model described in the previous section to be unstable to HP mode type disturbances. Once again, we see that there is a very close agreement, and now we also see the predicted transition to smaller wavenumber as R decreases. Though not plotted here, near the end of the experiment, as R became very small, we occasionally observed very widely spaced cusps, with substantially smaller, though still positive, phase speed. These corresponded well with the predictions for RP mode.

Finally, and analogously to the HP mode, downward cusping of the lower density interface was found to be associated with the presence of a region of overturning in the lower layer. In figure 7, we show that the wavenumber of these disturbances agrees well with the model predictions for HM modes, and thus these overturnings should be thought of as finite amplitude manifestations of the HM mode. Once again, for very small R, RM modes

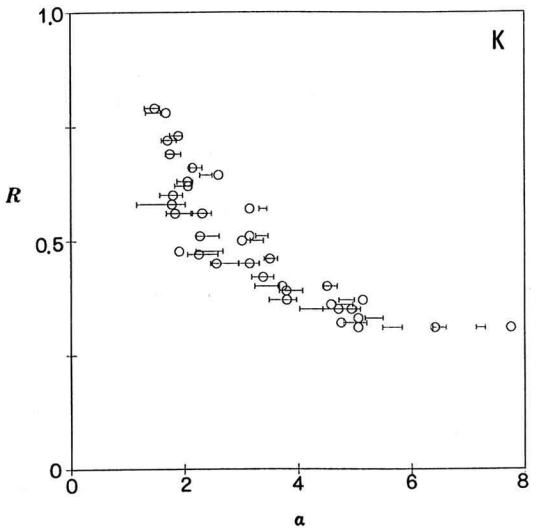

Figure 5: Wavenumber of observed K mode overturnings (circles) for various R. The error bars represent the theoretical predictions of (1), taking into account the other applicable parameters. Note the transition to larger alpha as R decreases.

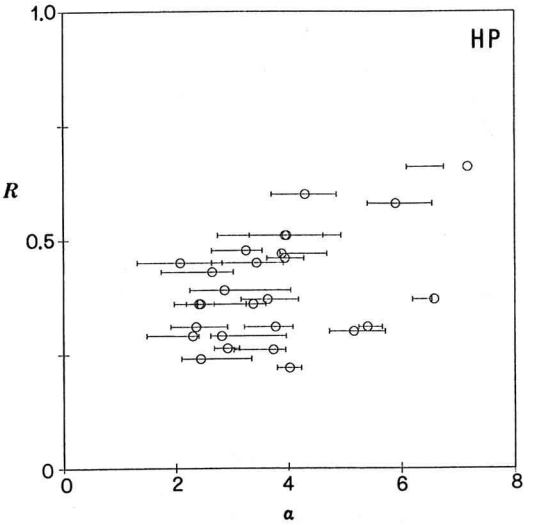

Figure 6: Wavenumber of observed HP mode overturnings (circles) for various R. The error bars represent the theoretical predictions of (1), taking into account the other applicable parameters. Note the transition to smaller alpha as R decreases.

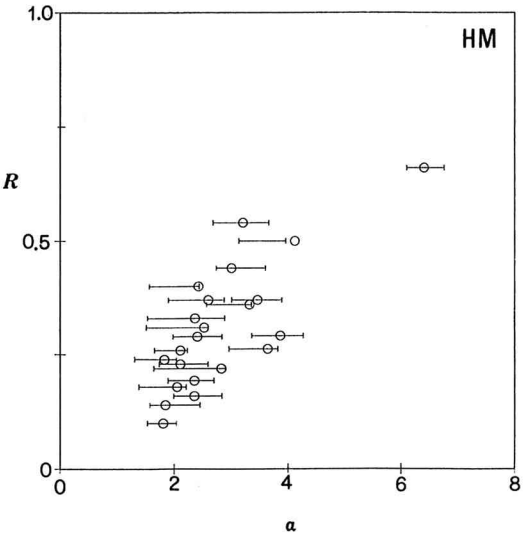

Figure 7: Wavenumber of observed HM mode overturnings (circles) for various R. The error bars represent the theoretical predictions of (1), taking into account the other applicable parameters. Note the transition to smaller alpha as R decreases.

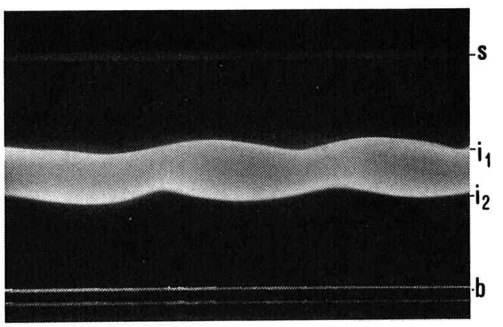

Photogragh 1: K mode type disturbances. s, i_1,i_2 and b correspond to surface, upper interface, lower interface and bed, respectively.

were observed.

The two Holmboe type modes often had significant three dimensionality early in their evolution, and were the major cause of mixing of within the flow. In particular, the mixing associated with HM modes was often sufficiently vigorous for another, fourth, layer to appear with density intermediate between ρ_3 and ρ_2.

When $R \sim 0.3$, all three instability types are observed simultaneously, for significant periods of time. However, depending on the values of Θ and β, linear theory predicts that one of the Holmboe type modes should totally dominate the evolution, and have a growthrate more than ten times that of the K mode. The observed behaviour may be due to a resonant triad of the three modes, whose conditions (namely $\alpha_K = \alpha_{HP} + \alpha_{HM}$, and $c_K = c_{HP} + c_{HM}$) are satisfied over a wide region of parameter space for the three linearly unstable modes.

3.Conclusions

A simple linear model well predicts the wavelengths and phase speeds of several forms of instability observed in a stratified shear flow. However the flow is susceptible to multiple simultaneous instabilities even when the predicted growthrates of the various observed modes vary by more than one order of magnitude. Thus this simple flow,that is likely to occur at river mouths, is explained qualitatively by linear theory. A nonlinear analysis must also be conducted to investigate the multiple modal structure at finite amplitude, as well as the (observed) different mixing effects of the instabilities.

This research was made possible by the support of the Japan Canada Project in Weather and Climate of the Arctic, and a grant-in-Aid for Scientific Research (B) of the Ministry of Education, Science and Culture, Japan under Grant No.04452231, 1992.

References

Caulfield C. P., 1991: *Ph. D. Thesis, University of Cambridge.*
Drazin P. G. and Reid W. H., 1981: *C. U. P.*
Holmboe J., 1962: *Geofys. Publ.* **24**, 67-113.
Lawrence G. A., Browand F. K. and Redekopp L. G., 1991: *Phys. Fluids* **A3**, 2360-2370.
Taylor G. I., 1931: *Proc. Roy. Soc.* **A132**, 499-523.
Yoshida S., 1986: *Bull. Faculty Eng. Hokkaido U.* 130 127-135.